A 424-year tree-ring based PDSI reconstruction of *Cedrus deodara* D. Don from Chitral HinduKush Range of Pakistan: linkages to the ocean oscillations

Sarir Ahmad[1, 2], Liangjun Zhu[1, 2], Sumaira Yasmeen[1, 2], Yuandong Zhang[3], Zongshan Li[4], Sami Ullah[5], Shijie Han[6, *], Xiaochun Wang[1, 2,*]

[1] Center for Ecological Research, Northeast Forestry University, Harbin 150040, China

[2] Key Laboratory of Sustainable Forest Ecosystem Management-Ministry of Education, School of Forestry, Northeast Forestry University, Harbin 150040, China

[3] Key Laboratory of Forest Ecology and Environment, State Forestry Administration, Institute of Forest Ecology, Environment and Protection, Chinese Academy of Forestry, Beijing 100091, China

[4] State Key Laboratory of Urban and Regional Ecology, Research Center for Eco-Environmental Sciences, Chinese Academy of Sciences, Beijing 100085, China

[5] Department of Forestry, Shaheed Benazir Bhutto University, Sheringal, Dir Upper, Pakistan

[6] State Key Laboratory of Cotton Biology, School of Life Sciences, Henan University, Kaifeng 475001, China

Corresponding authors: Xiaochun Wang, E-mail: wangx@nefu.edu.cn and Shijie Han, E-mail: hansj@iae.ac.cn

Abstract. Currently, the rate of global warming has led to persistent drought patterns. It is considered to be the preliminary reason affecting socio-economic development under the background of dynamic forecasting of water supply and forest ecosystems in West Asia.

However, long-term climate records in the semi-arid Chitral Mountains of northern Pakistan are seriously lacking. Therefore, we developed a new tree-ring width chronology of *Cedrus deodara* spanning the period of 1537-2017. We reconstructed the March-August Palmer Drought Sensitivity Index (PDSI) for the past 424 years back to A.D. 1593. Our reconstruction was featured with nine dry and eight wet periods 1593-1598, 1602-1608, 1631-1645, 1647-1660, 1756-1765, 1785-1800, 1870-1878, 1917-1923, 1981-1995, and 1663-1675, 1687-1708, 1771-1773, 1806-1814, 1844-1852, 1932-1935, 1965-1969 and 1996-2003, respectively. This reconstruction is consistent with other dendroclimatic reconstructions in west Asia, confirming its reliability. The analysis of multi-taper method and wavelet analysis revealed drought variability at periodicities of 2.1-2.4, 3.3, 6, 16.8, and 34-38 years. The drought patterns could be linked to the broad-scale atmospheric-oceanic variability such as El Niño-Southern Oscillation (ENSO), Atlantic Multi-decadal Oscillation (AMO) and solar activity. In terms of current climate conditions, our findings have important implications for developing drought-resistant policies in communities on the fringes of Hindu Kush mountain Ranges in northern Pakistan.

Keywords: Tree rings, Growth-climate response, Drought variability, ENSO, dendroclimatology, the broad-scale atmospheric-oceanic variability

1. Introduction

Numerous studies have shown that the intensity and frequency of drought events have increased due to rapid climate warming (IPCC, 2013; Trenberth et al., 2014). The apparent drought has had serious adverse effects on social, natural, and economic systems (Ficklin et al., 2015; Yao and Chen, 2015; Tejedor et al., 2017; Yu et al., 2018). Global drought is considered to be the most destructive climate disaster that has caused billions of dollars in worldwide loss (van der Schrier et al., 2013; Lesk et al., 2016).

Pakistan has a semi-arid climate, and its agriculture economy is most vulnerable to drought (Kazmi et al., 2015; Miyan, 2015). The long-term drought from 1998 to 2002 reduced agricultural production, with the largest reduction in wheat, barley and sorghum (from 60% to 80%) (Ahmad et al., 2004). ~~The n~~northern Pakistan is considered to ~~be~~ the world's largest ~~area of~~ irrigation network (Treydte et al., 2006). The production and life of local residents are strongly dependent on monsoon precipitation ~~brought by the mighty~~ ocean and atmospheric circulation system, including El Niño Southern Oscillation (ENSO), Atlantic Multi-decadal Oscillation (AMO), Pacific Decadal Oscillation (PDO) and others (Treydte et al., 2006; Cook et al., 2010; Miyan, 2015; Zhu et al., 2017). However, the current warming rate has changed ~~the~~ regional hydrological conditions, leading to an unsustainable water supply (Hellmann et al., 2016; Wang et al., 2017). It is not only critical for agricultural production but also leads to forest mortality, vegetation loss (Martínez-Vilalta and Lloret, 2016) and increases the risk of wildfires (Turner et al. 2015; Abatzoglou and Williams 2016). The degradation of grassland and loss of livestock caused by drought ~~eventually~~ affect the lifestyle of nomadic peoples, especially in high-altitude forested areas (Pepin et al., 2015; Shi et al., 2019).

The Hindu Kush Himalayan region (HKH) is the source of ten major rivers in Asia, which provides water resources for one fifth of the world's population (Rasul, 2014; Bajracharya et al., 2018). The region is particularly prone to drought, floods, avalanches and landslides, with more than 1 billion people exposed to increasing frequency and serious risks of natural disasters (Immerzeel et al., 2010; Immerzeel et al., 2013). The extent of climate change in this area is significantly higher than the world average, which has seriously threatened the safety of life and property, traffic and other infrastructure in the downstream and surrounding areas (Lutz et al., 2014). Dry conditions are exacerbated by an increase in the frequency of heatwaves in recent decades (Immerzeel et al., 2010; IPCC, 2013). The intensity and frequency of drought ~~trend~~ are very complex in HKH, and there is no manifest measuring tool to compute how long ~~the~~ drought period might persist. Climate uncertainty complicates the situation, for example, ~~whether~~ the drought trend is increasing or decreasing (Chen et al., 2019). Most studies ~~believe~~ that the wetting trend in HKH is going to ~~increase in current~~ decades (Treydte et al., 2006). However, some extreme drought events in the region ~~are~~ very serious and persistent (Gaire et al., 2017). Little has been done to examine the linkage between drought trend and large-scale ocean climate drivers (Cook et al., 2003; Gaire et al., 2017). ~~Besides~~ in northern Pakistan, ~~there is little research on the dendroclimatology and~~ instrumental climate records are inadequate in terms of quality and longevity (Treydte et al., 2006; Khan et al., 2019). In high altitude, arid and semi-arid areas, forest growth more sensitive to climate change, so dare need to understand more about the long-term drought regimes of the past (Wang et al., 2008). Climate reconstruction is the best way to understand long-term climate change and expand climate record to develop forest management strategies. Researchers used multiple proxies, including ice cores, speleothems, lake sediments, and historical documents and tree rings to reconstruct past short-term or long-term climate change. In addition, tree rings were widely used in long-term paleoclimatic reconstructions and forecasting future climate because of their accurate dating, high resolution, wide distribution, easy access, long time series, and abundant environmental information recorded (Esper et al., 2016; Zhang et al., 2015; Klippel et al., 2017; Shi et al., 2018; Chen et al., 2019)

In this study, we collected drought-sensitive tree-ring cores of *Cedrus deodar* from the upper and lower HKH region of Pakistan. These tree rings have a good potential for dendroclimatic study

(Yadav, 2013). Then, the March-August Palmer Drought Sensitivity Index (PDSI) was reconstructed for the past 424 years to examine the climatic variability and driving forces. To verify its reliability, we compared our reconstructed PDSI with other available paleoclimatic records (Treydte et al., 2006) near our research area. The intensity and drought mechanism in this area were also discussed. This will be the first time that the drought index has been reconstructed in northern Pakistan and is considered to be a baseline for more tree-ring reconstruction in Pakistan.

2 Material and Methods

2.1 Study area

We conducted our research in the Chitral, Hindu-Kush (HK) Mountains of northern Pakistan (35.36^{o} N, 71.48^{o} E, Fig. 1). Northern Pakistan is a subtropical monsoon climate. Summer is dry and hot, spring is wet and warm, and in some high altitudes, it snows all the year-round. March is the wettest month (with an average precipitation of 107 mm), while July or August is the driest (with an average precipitation of 6.3 mm). July is the hottest month (mean monthly temperature 36 ^{o}C), and January is the coldest (mean monthly temperature -0.8 ^{o}C) (Fig. 2). The soil at our sampling sites is acidic, with little variation among a stand of forest. Similarly, the soil water holding capacity ranged from 47%±2.4% to 62%±4.6%, while the soil moisture ranged from 28%±0.57% to 57%±0.49% (Khan et al., 2010). Chitral forest is mainly composed of *Cedrus deodara*, *Juglans regia*, *Juniperus excelsa*, *Quercus incana*, *Q. diltata*, *Q. baloot* and *Pinus wallichiana*. *C. deodara* was selected for sampling because of the high dendroclimatic value (Khan et al., 2013).

Climate data such as monthly precipitation and temperature (1965-2016) were obtained from the meteorological station of Chitral in northern Pakistan. PDSI downloaded from the datasets of the nearest grid point (35.36° N, 71.48° E) through Climatic Research Unit (CRU TS.3.22, 0.5° latitude × 0.5° longitude). The most common reliable period spanning from 1965 to 2016 was used (http://climexp.knmi.nl/) for dendroclimatic studies (Harris et al., 2014; Shekhar, 2015).

The Atlantic Multi-decadal Oscillation (AMO) index was downloaded from KNMI Climate Explorer https://climexp.knmi.nl/data/iamo_hadsst.dat over the period 1890-2016. The reconstructed June-August South Asia Summer Monsoon (JJA-SASM) data was downloaded from Monsoon Asia Drought Atlas (MADA) http://drought.memphis.edu/MADA/TimeSeriesDisplay.aspx over the period 1300-2005.

2.2 Tree rings collection and chronology development

Tree-ring cores collected in Chitral forest from *C. deodara* trees, located in the northern area of Pakistan. To maintain the maximum climatic signals contained in tree rings, undisturbed open canopy trees were selected. One core per tree at breast height (~1.3 m above ground) was sampled using a 5.15 mm diameter increment borer (Haglöf Sweden, Langsele, Sweden). In addition, several ring-width series were also downloaded from the International Tree-Ring Data Bank from the Bumburet forest and Zairat forest (https://www.ncdc.noaa.gov/paleo-search/) collected in 2006 (Fig. 1).

All tree-ring samples were first glued than progressively mounted, dried, and polished according to a set procedure (Fritts, 1976; Cook and Kairiukstis, 1990). The preceding calendar year was assigned and properly cross-dated. False rings were identified by Skeleton-plot and cross dated as mentioned in Stokes and Smiley (1968).

The cores were measured using the semi-automatic Velmex measuring system (Velmex, Inc., Bloomfield, NY, USA) with an accuracy of 0.001 mm. The COFECHA program was then used to check the accuracy of cross-dating and measurement (Holmes, 1983). All false one has been modified and the cores that didn't match the master chronology were not used to develop tree-ring chronology. For quality checks, the COFECHA 2002 program was used. (Holmes, 1998). The synthesized tree-ring width chronology (Fig. 3) was built by the program R (Zang and Biondi, 2015). To preserve climate signals and avoid noise, appropriate detrending was introduced. Biological trends of tree growth associated with tree age were conservatively detrended by fitting negative exponential curves or linear lines (Fritts, 1976). The tree-ring chronology was truncated where the expressed population signal (EPS) was large than 0.85, which is a generally accepted standard for more reliable and potential climate signal results (Wigley et al., 1984; Cook and Kairiukstis, 1990). The mean correlation between trees (Rbar), means sensitivity (MS) and EPS was calculated to evaluate the quality of chronology (Fritts, 1976). Higher mean sensitivity and EPS were considered to be a strong response to climate change (Cook and Kairiukstis, 1990).

2.3 Statistical analysis

Correlation analysis was conducted between tree-ring indexes (TRI) and monthly temperature, precipitation, and PDSI (from previous June to current September, collected from the nearby stations or downloaded from KNMI). Then, the PDSI was reconstructed according to the relationship between TRI and climate variables. To test the validity and reliability of our model, reconstruction was checked by the split-period calibration/verification methods subjected to different statistical parameters, including reduction of error (RE), coefficient of efficiency (CE), Pearson correlation coefficient (*r*), R-square (R^2), product mean test (PMT), sign test (ST) and Durban-Watson test (DWT) (Fritts, 1976). PMT is used to test the level of consistency between the actual and estimated values, taking into account the signs and magnitudes of departures from the calibration average (Fritts, 1976). ST expresses the coherence between reconstructed and instrumental climate data by calculating the number of coherence and incoherence, which is often used in previous studies (Fritts, 1976; Cook et al., 2010). DWT is used to calculate first-order autocorrelation or linear trend in regression residuals (Cook and Pederson, 2011; Wiles et al., 2015). The RE and CE larger than zero were considered skills (Fritts, 1976; Cook et al., 1999).

According to the reference of Chen et al. (2019), we defined the wet or dry years of our reconstruction with the PDSI value greater than or less than the mean ±1 standard deviation. The mean ±1 standard deviation is easy to calculate the dry and wet years, which has been observed in different tree-ring PDSI reconstructions (Wang et al., 2008; Chen et al., 2019). We assessed the dry and wet periods for many years based on strength and intensity.

Although there were few reconstructions in our study area, we compared our reconstruction with other available drought reconstructions near the study area (Treydte et al., 2006). The multi-taper method (MTM) was used for spectral analysis, and the Wavelet analysis was used to determine the statistical significance of band-limited signals embedded in red noise by providing very high-resolution spectral estimates that eventually give best possible option against leakage. To identify the local climate change cycle, the background spectrum was used (Mann and Lees, 1996).

3 Results

3.1 Main climate limiting factors for Cedrus deodar

The statistical parameters of the tree-ring chronologies, including MS (0.16), Rbar (0.59), and EPS (0.94) indicated that there were enough common signals in our sampled cores, and our chronology is suitable for dendroclimatic study. According to the threshold of EPS (EPS > 0.85), 1593-2016 was selected as the reconstruction period to truncate the period 1537-1593 of the chronology (Fig. 3).

The TRI was significantly positively correlated with monthly PDSI (p<0.01) (Fig. 4a). However, the TRI was positively correlated with the precipitation in October of the previous year and February-May of the current year, and negatively correlated with the precipitation in September of the previous year (p<0.001). The TRI was significantly positively (p < 0.001) with the minimum temperature in September and December of the previous year and January and February of the current year (Fig. 4b). Similarly, the TRI was significantly negatively (p < 0.001) correlated the maximum temperature in January, October and December of the previous year and February-June of the current year. The TRI was only significantly positively correlated the maximum temperature in September (Fig. 4b).

3.2 Reconstruction of the past drought variation in northern Pakistan

The correlation between and TRI was the highest from March to August, indicating that the growth of *C. deodara* was most strongly affected by the drought before and during the growing season. Based on the above correlation analysis results, the March-August PDSI was the most suitable for seasonal reconstruction. The linear regression model between TRI and mean March-

August PDSI for the calibration period from 1960 to 2016 was significant (F=52.4, p <0.001, adjusted R^2 = 0.49, r =0.70). The regression model was:

$$Y = 5.1879x - 5.676$$

Where Y is the mean March-August PDSI and x is the tree-ring index.

The split calibration-verification test showed that the variance explained was higher during the two calibration periods (1960-1988 and 1989-2016). For the calibration period (1960-2016), the reconstruction accounted for 39.2% of the scPDSI variation (37.6 after accounting for the loss of degrees of freedom). Statistics of R, R^2, ST, and PMT are all significant at p <0.05, indicating that the model was reliable (Table 1). The RE and CE has a theoretical range of -∞ to +1, but the benchmark for determining skill is the calibration and verification period mean. Therefore, a RE >0 and CE >0 indicates reconstruction skill in excess of climatology (Cook et al., 1999). Here, the most rigorous RE and CE tests in the verification period were all positive. Hence, these results made the model more obvious and robust in PDSI reconstruction.

The instrumental and reconstructed scPDSIs of the Hindu Kush Mountains had similar trends and parallel calibrations during short- and long-time scales in the 20th century (Fig. 5). However, the reconstructed scPDSI did not fully capture the magnitude of extremely dry or wet conditions.

3.3 The drought regime in the Chitral Mountain, northern Pakistan for the past 424 years

Fig. 5 showed the dry and wet years of the past 424 years (1593-2016) in the Chitral Mountain in northern Pakistan. The dry periods were recorded in 1593-1598, 1602-1608, 1631-1645, 1647-1660, 1756-1765, 1785-1800, 1870-1878, 1917-1923, and 1981-1995. Similarly, the wet periods were recorded in 1663-1675, 1687-1708, 1771-1173, 1806-1814, 1844-1852, 1932-1935, 1965-1969, and 1996-2003.

To verify the accuracy and reliability of our reconstruction, we compared our results with the nearby precipitation reconstruction of Treydte et al. (2006) (Fig. 6). In the reconstruction of Treydte et al. (2006), the high and low raw $\delta^{18}O$ value represents dry and wet conditions, respectively, just opposite to the PDSI index. In most periods, our PDSI reconstruction and the precipitation reconstruction of Treydte et al. (2006) showed good consistency (Fig. 6). However, in some periods, they also showed inconsistent or even opposite changes in drought reconstruction. For example, in 1865-1900, the reconstruction of Treydte et al. (2006) was very wet, while our reconstruction was normal. In periods 1800-1810 and 1694-1702, the reconstruction of Treydte et al. (2006) was very dry, but our reconstruction was wet (Fig. 6).

Spectral analysis showed that the historical PDSI changes in the Hindukush Mountains showing several significant (95% or 99% confidence level) with periods at 33-38 (99%), 16.8 (99%), 2-3 (99%) years, corresponding to significant periodic peaks (Fig. 7).

The spatial correlation analysis between our reconstructed and actual PDSI from May to August shows that our drought reconstruction is a good regional representative (Fig. 8). This shows that our reconstruction is reliable and can reflect the drought situation in the region. In addition, the PDSI of low-frequency (the 31-year moving average) reconstruction had good consistency with AMO ($r = 0.53$, $p < 0.001$, 1890-2001) and SASM ($r = 0.35$, $p < 0.001$, 1608-1990), which indicated that these are the potential factors affecting the drought pattern in the region.

4 Discussion

4.1 Drought variation in Chitral HinduKush Range of Pakistan

The growth-climate relationship revealed the positive and negative influence of precipitation and summer temperature on growth. It means that water availability (PDSI) is the main limiting factor affecting the growth of *C. deodara*. Singh et al. (2006) reported that the previous October precipitation limited the growth of *C. deodara*, while Ahmed et al. (2011) found no such effect. Except for last August, November, and current September, maximum temperature has a negative impact on the growth of *C. deodara*, while the minimum temperature does not. These results suggest that moisture conditions in April-July are critical to the growth of *C. deodar* in the study area (Borgaonkar et al., 1996; Hussain et al., 2007; Khan et al., 2013). Remarkably, Chitral does not receive monsoon rains. That's why it is hard to understand how trees respond to different moisture trends.

Here we developed a 467-year (1550-2017) of tree ring chronology of *C. deodara*, and reconstructed the 424-year (1593-2016) drought variability of the Chitral Hindukush Range in northern Pakistan. The point years (narrow rings), 2002, 2001, 2000, 1999, 1985, 1971, 1962, 1952, 1945, 1921, 1917, 1902 and 1892, were recorded in our tree-ring record. The narrow ring formation occurs when extreme drought stress reduces cell division (Fritts et al., 1976; Shi et al., 2014). Therefore, the narrow rings are also consistent with the extreme drought years. Among them, 2001, 1999, 1952, and 1921 were identified by previous studies (Esper et al., 2003; Ahmed et al. 2010; Zafar et al., 2010; Khan et al., 2013; He et al., 2018). Sigdel and Ikeda (2010) reported that droughts occurred in 1974, 1977, 1985, 1993, and the winter of 2001 and the summers of 1977, 1982, 1991, and 1992. Our PDSI reconstruction fully captured the widespread drought in Pakistan, Afghanistan, and Tajikistan in 1970-1971 (Yu et al., 2014). The above drought has disrupted the people's daily life, leading to food and water shortages and livestock losses in high altitude areas (Yadav, 2011; Yadav and Bhutiyani, 2013; Yadav et al., 2017). This drought may also be due to the failure of Western disturbance precipitation (Hoerling et al., 2003).

In Fig. 5, the mean of our reconstructed PDSI is below zero. There are two possible reasons for this phenomenon. First, tree growth is more sensitive to drying than to wetting. As a result, more drought information is recorded in ring widths. This leads to a drier (less than zero) PDSI reconstructed with tree rings. This phenomenon exists in many tree-ring PDSI reconstructions (Hartl-Meier et al., 2017; Wang et al., 2008). Second, the period (1960-2016) used to reconstruct the equation is relatively dry. This cause the mean of the reconstruction equation to be lower than zero (dry), resulting in lower values for the whole reconstructions. Therefore, when applying the PDSI data reconstructed by tree rings, its relative value is relatively reliable, and the absolute value data can only be used after adjustment. The adjustment method of the absolute value needs to be further studied.

Our reconstruction also captured a range of climate changes mentioned in other studies (Ahmad et al., 2004; Yu et al., 2014; Chen et al. 2019; Gaire et al., 2019). Our dry periods (1981-1987, 1870-1875 to 1761-1764) were consistent with the results of Chen et al. (2019). The dry period 1645-1631 also reported in tree-ring based drought variability of Silk Road (Yu et al., 2014). Most notably, three mega drought events in Asian history (Yadav, 2013; Panthi et al., 2017; Gaire et al., 2019), namely, the Strange Parallels drought (1756-1768), the East India drought (1790-1796) and late Victorian Great Drought (1876 to 1878) was clearly recorded in our reconstructed PDSI. Based on the above results, drought changes in Northern Pakistan and the central Himalayas are closely related to large-scale ocean-atmospheric circulation and synchronous in western Asia (Gaire et al., 2019). The driest period of 1917-1921 of our reconstruction, followed by another dry period 1784-1802, coincided with the eruption of Laki volcano (Iceland) in 1783. This could mean that widespread drought on the continent could be linked to volcanic eruptions (Chen et al., 2019). Interestingly, the wet period of 1995-2016 was very consistent with those of Yadav et al. (2017). These results suggested that the long-term continuous wets in 31 years of the past 576 years (1984-2014) may have increased the mass of glaciers in the northwest Himalaya and Karakoram (Cannon et al., 2014). The devastating floods of July 2010 were also captured by our reconstruction, affecting about a fifth of Pakistan (20 million peoples) (Yaqub et al., 2015). Therefore, we speculate that the size of the Hindukush glacier and the mass of glaciers near our study areas will continue to increase if it continues to get wet.

Our PDSI reconstruction and the precipitation reconstruction of Treydte et al. (2006) showed a strong consistency (Fig. 6), which proves that our reconstruction is reliable. The inconsistency between them in some periods may be because the PDSI is affected by temperature and may not be completely consistent with precipitation (Li et al., 2015). The inconsistency between the reconstruction of ring width and oxygen isotope in some periods may also be due to the different response of radial growth and isotope to disturbance (McDowell et al., 2002). In addition, the lack of consistency between different data sets or regions may be due to the dominance of internal climate variability over the impact of natural exogenous forcing conditions on multi-decadal timescales (Bothe et al., 2019).

4.2 The linkage of drought variation with the ocean oscillations

The results of wavelet and MTM analysis indicated that the low and high-frequency periods of drought in northern Pakistan may teleconnection with both large-small scale climate oscillation (Fig. 7). The spatial correlation exhibited the significant similarity of El Niño-Southern Oscillation (ENSO) in the region (Fig. 8). The intensity of India monsoon in this area was modulated by ENSO patterns. The high frequency of drought cycle (2.1-3.3 years) may be related to the ENSO (van Oldenborgh and Burgers, 2005). Khan et al. (2014) showed that most of our study area is covered by monsoon shadow, but the Asian monsoon showed an overall weak trend in recent decades (Wang and Ding, 2006; Ding et al., 2008). Therefore, the increase of regional precipitation may be linked to the ENSO. Previous studies (Wang et al., 2006; Palmer et al., 2015; Shi et al., 2018; Chen et al., 2019) have confirmed that ENSO is an important factor in regulating the hydrological conditions related to the AMO. In the past, sever famine and drought occurred simultaneously with the warm phase of ENSO, and these events were related to the failure of Indian Summer Monsoon (Shi et al., 2014).

The middle-frequency cycle (16 years) may be related to the solar cycle, which is similar to other studies in South Asia (Panthi et al., 2017; Shekhar et al., 2018; Chen et al., 2019). Solar activity may affect climate fluctuations in the Chitral, Hindukush ranges, northern Pakistan (Gaire et al., 2017). The low-frequency (36-38 years) may be caused by the Atlantic Multi-decadal Oscillation (AMO), which is the anomalies of sea surface temperatures (SST) in the North Atlantic basin. Previous studies have shown that the AMO may alter drought or precipitation patterns in North America (Mccabe et al., 2004; Nigam et al., 2011) and Europe (Vicente-Serrano and López-Moreno, 2008). Although our study area is far from the Atlantic Ocean, it may also be affected by AMO (Lu et al., 2006; Wang et al., 2011; Yadav, 2013). Lu et al. (2006) found that the SST anomalies in the North Atlantic (such as AMO) can affect the Asian summer monsoon. Goswami et al. (2006) reported the mechanism for the AMO influence on the Indian monsoon precipitation. The warm AMO appears to cause a late withdrawal of the

Indian monsoon through strengthening the meridional gradient of tropospheric temperature in autumn (Goswami et al., 2006; Lu et al., 2006). Yadav (2013) suggested that the role of AMO in modulating winter droughts over the western Himalaya through the tropical Pacific Ocean. Wang et al. (2009) pointed out that the AMO heat the Eurasian middle and upper troposphere in all four seasons, resulting in weakened Asian winter monsoons but enhanced summer monsoons. This is consistent with the findings that the AMO affecting climate in China, which is made possible by the Atlantic-Eurasia wave train from the North Atlantic and increased due to global warming (Qian et al., 2014). Further work is still needed to unravel the links between the Pacific and Atlantic Oceans and how the two are coupled through the atmosphere and oceans to affect drought in Asia.

Dimri (2006) found that the precipitation surplus in winter from 1958 to 1997 was related to the significant heat loss in the northern Arabian Sea, mainly due to intensification of water vapor flow in the west and the enhancement of evaporation. As a result, large-scale changes in Atlantic temperature could also regulate western Asia climate. Our result was supported by other dendroclimatic studies (Sano et al., 2005; Chen et al., 2019). Precipitation in Mediterranean, Black sea (Hatwar et al., 2005; Giesche et al., 2019), and parts of northern Pakistan showed an upward trend from 1980 to 2010, but the precipitation in the Chitral Mountains received from Winter Indian Monsoon (WID) (December-March) and the rain shadows in summer (Khan et al., 2013). Predicting different climate cycle patterns is not easy. Besides, the flow of the Upper Indus Basin (UIB) depends on changes in the Ablation air mass (Rashid et al., 2018; Rao et al., 2018), so small changes in the Ablation mass may eventually lead to changes in water quality and quantity. The UIB is considered as a water tower in the plain (Immerzeel et al., 2010), so the

Hindukush Mountains are particularly important for extending the proxy network to improve understanding of different climatic behaviors.

Due to reconstruction indices, species, geographical differences and other reasons, it does not remain the same with the whole period. The drought regimes in Hindukush ranges in northern Pakistan may be linked to regional, local, and global climate change. We only studied the response of *C. deodara* to different climate change in the Chitral region, northern Pakistan. Therefore, we suggest further high-resolution and well-dated record are needed to augment dendroclimatic network in the region.

5 Conclusion

Based on the significance of the tree-ring width of *C. deodara*, we developed a 467-years chronology (1550-2017). Considering that EPS threshold is greater than 0.85 (> 5 trees), we reconstructed the current March-August PDSI from 1593 to 2016. Our reconstruction captured different drought changes in different time scale in the Chitral, Hindukush Mountain, Pakistan, which falls in the Indus civilization. Several studies have shown that the Indus civilization changed dramatically in history because of its unpleasant climate. Three historic mega drought events, the Strange Parallel Droughts (1756-1768) the East Indian Drought (1790-1796) and late Victorian Great Drought (1876-1878) were captured by our reconstructed PDSI. These large scales and small droughts may be caused by cold or hot climate. Our results are consistent with other dendroclimatic records, which further support the feasibility of our reconstruction. Besides, due to a different climate change patterns in the region, we suggested extending the different proxy networks to understand the remote teleconnection across the continent on the multi-decadal to centennial timescales to meet future climate challenges.

Acknowledgments

This research was supported by the Key Project of the China National Key Research and Development Program (2016YFA0600800), the Fundamental Research Funds for the Central Universities (2572019CP15 and 2572017DG02), the Open Grant for Eco-meteorological Innovation Laboratory in northeast China, China Meteorological Administration (stqx2018zd02), and the Chinese Scholarship Council. We appreciate the staff of the International Office, Northeast Forestry University for their excellent services. We thank Dr. Muhmmad Usman, Mr. Shahid Humayun Mirza and Dr. Nasrullah Khan for their communications in revising the manuscript. We also appreciate Mr. Muhmmad Arif, Sher Bahder, Wali Ullah and Mushtaq Ahmad for their great help in the fieldwork.

Data availability

The reconstructed PDSI can be obtained from the supplementary file of this paper. The tree-ring width used in this paper can be download from the International Tree-ring Data Bank.

Author contributions

Xiaochun Wang and Sarir Ahmad initiated this idea. Sarir Ahmad and Sami Ullah collected samples in the field. Liangjun Zhu and Sumaira Yasmeen crossdated and measured the samples. Sarir Ahmad and Xiaochun Wang wrote the manuscript. Liangjun Zhu, Yuandong Zhang, Zongshan Li and Shijie Han revised the manuscript.

Competing interest

The authors declare that they have no conflict of interest.

References

Abatzoglou, J. T., and Williams, A. P.: Impact of anthropogenic climate change on wildfire across western US forests, Proceedings of the National Academy of Sciences, 113, 11770-11775, 2016.

Ahmed, M., Khan, N., and Wahab, M.: Climate response function analysis of *Abies pindrow* (Royle) Spach. preliminary results, Pakistan Journal of Botany, 42, 165-171, 2010.

Ahmed, M., Shaukat, S. S., and Siddiqui, M. F.: A multivariate analysis of the vegetation of *Cedrus deodara* forests in Hindu Kush and Himalayan ranges of Pakistan: evaluating the structure and dynamics, Turkish Journal of Botany, 35, 419-438, 2011.

Ahmad, S., Hussain, Z., Qureshi, A. S., Majeed, R., and Saleem, M.: Drought mitigation in Pakistan: current status and options for future strategies, Working Paper 85. Colombo, Sri Lanka: International Water Management Institute, 2004.

Bajracharya, A. R., Bajracharya, S. R., Shrestha, A. B., and Maharjan, S. B.: Climate change impact assessment on the hydrological regime of the Kaligandaki Basin, Nepal, Science of the Total Environment, 625, 837-848, 2018.

Borgaonkar, H., Pant, G., and Rupa Kumar, K.: Ring-width variations in *Cedrus deodara* and its climatic response over the western Himalaya, International Journal of Climatology: A Journal of the Royal Meteorological Society, 16, 1409-1422, 1996.

Bothe, O., Wagner, S., and Zorita, E.: Inconsistencies between observed, reconstructed, and simultaed precipitation indices for England since the year 1650 CE, Climate of the Past, 15, 307-334, 2019.

Cannon, F., Carvalho, L. M. V., Jones, C., and Bookhagen, B.: Multi-annual variations in winter westerly disturbance activity affecting the Himalaya. Climate Dynamics, 44, 441-455, 2015.

Chen, F., Zhang, T., Seim, A., Yu, S., Zhang, R., Linderholm, H. W., Kobuliev, Z. V., Ahmadov, A., and Kodirov, A.: Juniper tree-ring data from the Kuramin Range (northern Tajikistan), reveals changing summer drought signals in western Central Asia. Forests, 10(6), 505, 2019.

Cook, E. R., Anchukaitis, K. J., Buckley, B. M., D'Arrigo, R. D., Jacoby, G. C., and Wright, W. E.: Asian monsoon failure and megadrought during the last millennium, Science, 328, 486-489, 2010.

Cook, E. R., Meko, D. M., Stahle, D. W., and Cleaveland, M. K.: Drough reconstruction for the continental United States, Journal of Climate, 12, 1145-1162, 1999.

Cook, E. R., and Pederson, N.: Uncertainty, emergence, and statistics in dendrochronology, in: Hughes, M. K., Swetnam, T. W., and Diaz, H. F., Dendroclimatology, Springer, Dordrecht, USA, 77-112, 2011.

Cook, E. R., and Kairiukstis, L. A.: Methods of dendrochronology: applications in the environmental sciences, Kuluwer Academic Publishers, Dordrecht, USA, 1990.

Cook, E. R., Krusic, P. J., and Jones, P. D.: Dendroclimatic signals in long tree-ring chronologies from the Himalayas of Nepal, International Journal of Climatology, 23, 707-732, 2003.

Dimri, A.: Surface and upper air fields during extreme winter precipitation over the western Himalayas, Pure and Applied Geophysics, 163, 1679-1698, 2006.

Esper, J., Shiyatov, S., Mazepa, V., Wilson, R., Graybill, D., and Funkhouser, G.: Temperature-sensitive Tien Shan tree ring chronologies show multi-centennial growth trends, Climate Dynamics, 21, 699-706, 2003.

Esper, J., Krusic, P. J., Ljungqvist, F. C., Luterbacher, J., Carrer, M., Cook, E., Davi, N. K., Hartl-Meier, C., Kirdyanov, A., and Konter, O.: Ranking of tree-ring based temperature reconstructions of the past millennium, Quaternary Science Reviews, 145, 134-151, 2016.

Ficklin, D. L., Maxwell, J. T., Letsinger, S. L., and Gholizadeh, H.: A climatic deconstruction of recent drought trends in the United States, Environmental Research Letters, 10, 044009, 2015.

Fritts, H. C.: Tree rings and climate. Academic Press, New York, USA, 1976.

Gaire, N. P., Bhuju, D. R., Koirala, M., Shah, S. K., Carrer, M., and Timilsena, R.: Tree-ring based spring precipitation reconstruction in western Nepal Himalaya since AD 1840, Dendrochronologia, 42, 21-30, 2017.

Gaire, N. P., Dhakal, Y. R., Shah, S. K., Fan, Z.-X., Bräuning, A., Thapa, U. K., Bhandari, S., Aryal, S., and Bhuju, D. R.: Drought (scPDSI) reconstruction of trans-himalayan region of central himalaya using *Pinus wallichiana* tree-rings, Palaeogeography, Palaeoclimatology, Palaeoecology, 514, 251-264, 2019.

Giesche, A., Staubwasser, M., Petrie, C. A., and Hodell, D. A.: Indian winter and summer monsoon strength over the 4.2 ka BP event in foraminifer isotope records from the Indus River delta in the Arabian Sea, Climate of the Past, 15, 73-90, 2019.

Goswami, B.N., Madhusoodanan, M.S., Neema, C.P., Sengupta, D.: A physical mechanism for North Atlantic SST influence on the Indian summer monsoon, Geophysical Research Letters, 33, L02706, 2006.

Harris, I., Jones, P. D., Osborn, T. J., and Lister, D. H.: Updated high-resolution grids of monthly climatic observations–the CRU TS3. 10 Dataset, International Journal of Climatology, 34, 623-642, 2014.

Hartl-Meier, C., Büntgen, U., Smerdon, J. E., Zorita, E., Krusic, P. J., Ljungqvist, F. C., Schneider, L., and Esper, J.: Temperature covariance in tree ring reconstructions and model simulations over the past millennium, Geophysical Research Letters, 44, 9458-9469, 2017.

Hatwar, H., Yadav, B., and Rao, Y. R.: Prediction of western disturbances and associated weather over Western Himalayas, Current Science, 88, 913-920, 2005.

He, M., Bräuning, A., Grießinger, J., Hochreuther, P., and Wernicke, J.: May–June drought reconstruction over the past 821 years on the south-central Tibetan Plateau derived from tree-ring width series, Dendrochronologia, 47, 48-57, 2018.

Hellmann, L., Agafonov, L., Ljungqvist, F. C., Churakova, O., Düthorn, E., Esper, J., Hülsmann, L., Kirdyanov, A. V., Moiseev, P., and Myglan, V. S.: Diverse growth trends and climate responses across Eurasia's boreal forest, Environmental Research Letters, 11, 074021, 2016.

Hoerling, M., and Kumar, A.: The perfect ocean for drought, Science, 299, 691-694, 2003.

Holmes, R.: Computer assisted quality control, Tree-ring Bulletin, 43, 69-78, 1983.

Hussain, F., Shah, S. M., and Sher, H.: Traditional resource evaluation of some plants of Mastuj, District Chitral, Pakistan, Pakistan Journal of Botany, 39, 339-354, 2007.

Immerzeel, W. W., P ellicciotti, F., and Bierkens, M. F. P.: Rising river flows throughout the twenty-first century in two Himalayan glacierized watersheds, Nature Geoscience, 6, 742-745, 2013.

Immerzeel, W. W., van Beek, L. P., and Bierkens, M. F.: Climate change will affect the Asian water towers, Science, 328, 1382-1385, 2010.

IPCC., Stocker, T.F., Qin, D., Plattner, G.K., Tignor, M., Allen, S.K., Boschung, J., Nauels, A., Xia, Y., Bex, V., Midgley, P.M. (Eds.), The Physical Science Basis.: Climate change, Contribution of Working Group I to the Fifth Assessment Report of the Intergovernmental Panel on Climate Change. Cambridge University Press, Cambridge and New York. 2013

Kazmi, D. H., Li, J., Rasul, G., Tong, J., Ali, G., Cheema, S. B., Liu, L., Gemmer, M., and Fischer, T.: Statistical downscaling and future scenario generation of temperatures for Pakistan region, Theoretical and Applied Climatology, 120, 341-350, 2015.

Khan, N., Ahmed, M., Wahab, M., and Ajaib, M.: Phytosociology, structure and physiochemical analysis of soil in *Quercus baloot* Griff, forest fistrict Chitral Pakistan, Pakistan Journal of Botany, 42, 2429-2441, 2010.

Khan, N., Ahmed, M., and Shaukat, S.: Climatic signal in tree-ring chronologies of *Cedrus deodara* from Chitral HinduKush Range of Pakistan, Geochronometria, 40, 195-207, 2013.

Klippel, L., Krusic, P. J., Brandes, R., Hartl-Meier, C., Trouet, V., Meko, M., and Esper, J.: High-elevation inter-site differences in Mount Smolikas tree-ring width data, Dendrochronologia, 44, 164-173, 2017.

Lesk, C., Rowhani, P., and Ramankutty, N.: Influence of extreme weather disasters on global crop rpoduction, Nature, 529, 84-87, 2016.

Li, Q., Liu, Y., Song, H., Yang, Y., and Zhao, B.: Divergence of tree-ring-based drought reconstruction between the individual sampling site and the Monsoon Asia Drought Atlas: an example from Guancen Mountain, Science Bulletin, 60(19), 1688-1697.

Lu, R., Dong, B., Ding, H.: Impact of the Atlantic Multidecadal Oscillation on the Asian summer monsoon, Geophysical Research Letters, 33, 194-199, 2006.

Lutz, A. F., Immerzeel, W. W., Shrestha, A. B., and Bierkens, M. F. P.: Consistent increase in high Asia's runoff due to increasing glacier melt and precipitation. Nature Climate Change, 4, 587, 2014.

McDowell, N., Brooks, J. R., Fitzgerald, S., and Bond, B. J.: Carbon isotope discrimination and growth response to stand density reductions in old *Pinus ponderosa* trees. Presented at 3rd International Conference on Applications of Stable isotope Techniques to Ecological Studies, Flagstaff, AZ, April 29-May 1, 2002.

Mann, M. E., and Lees, J. M.: Robust estimation of background noise and signal detection in climatic time series, Climatic Change, 33, 409-445, 1996.

Martínez-Vilalta, J., and Lloret, F.: Drought-induced vegetation shifts in terrestrial ecosystems: the key role of regeneration dynamics, Global and Planetary Change, 144, 94-108, 2016.

Mccabe, G.J., Palecki, M.A., Betancourt, J.L.: Pacific and Atlantic Ocean influences on multidecadal drought frequency in the United States, Proceedings of the National Academy of Sciences of the United States of America 101, 4136-4141, 2004.

Miyan, M. A.: Droughts in Asian least developed countries: vulnerability and sustainability, Weather and Climate Extremes, 7, 8-23, 2015.

Nigam, S., Guan, B., Ruiz-Barradas, A.: Key role of the Atlantic Multidecadal Oscillation in 20th century drought and wet periods over the Great Plains, Geophysical Research Letters, 38, 239-255, 2011.

Palmer, J. G., Cook, E. R., Turney, C. S., Allen, K., Fenwick, P., Cook, B. I., O'Donnell, A., Lough, J., Grierson, P., and Baker, P.: Drought variability in the eastern Australia and New Zealand summer drought atlas (ANZDA, CE 1500–2012) modulated by the Interdecadal Pacific Oscillation, Environmental Research Letters, 10, 124002, 2015.

Panthi, S., Bräuning, A., Zhou, Z.-K., and Fan, Z.-X.: Tree rings reveal recent intensified spring drought in the central Himalaya, Nepal, Global and Planetary Change, 157, 26-34, 2017.

Pepin, N., Bradley, R., Diaz, H., Baraer, M., Caceres, E., Forsythe, N., Fowler, H., Greenwood G, Hashmi, M. Z., Liu, X. D., Miller, J. R., Ning, L., Ohmura, A., Palazzi, E., Rangwala, I., Schöner, W., Severskiy, I., Shahgedanova, M., Wang, M. B., Williamson, S. N., and Yang D. Q.: Elevation-dependent warming in mountain regions of the world, Nature Climate Change, 5, 424-430, 2015.

Qian, C., Yu, J., Chen, G.: Decadal summer drought frequency in China: the increasing influence of the Atlantic Multi-decadal Oscillation, Environmental Research Letters 9, 124004, 2014.

Rao, M. P., Cook, E. R., Cook, B. I., Palmer, J. G., Uriarte, M., Devineni, N., Lall, U., D'Arrigo, R. D., Woodhouse, C. A., and Ahmed, M.: Six centuries of upper Indus Basin streamflow variability and its climatic drivers, Water Resources Research, 54, 5687-5701, 2018.

Rashid, M. U., Latif, A., and Azmat, M.: Optimizing irrigation deficit of multipurpose Cascade reservoirs, Water Resources Management, 32, 1675-1687, 2018.

Rasul, G.: Food, water, and energy security in South Asia: A nexus perspective from the Hindu Kush Himalayan region, Environmental Science & Policy, 39, 35-48, 2014.

Sano, M., Furuta, F., Kobayashi, O., and Sweda, T.: Temperature variations since the mid-18th century for western Nepal, as reconstructed from tree-ring width and density of Abies spectabilis, Dendrochronologia, 23, 83-92, 2005.

Shekhar, M.: Application of multi proxy tree ring parameters in the reconstruction of climate vis-à-vis glacial fluctuations from the eastern Himalaya, University of Lucknow, Lucknow, India, 2015.

Shekhar, M., Pal, A. K., Bhattacharyya, A., Ranhotra, P. S., and Roy, I.: Tree-ring based reconstruction of winter drought since 1767 CE from Uttarkashi, Western Himalaya, Quaternary International, 479, 58-69, 2018.

Shi, F., Li, J., and Wilson, R. J.: A tree-ring reconstruction of the South Asian summer monsoon index over the past millennium, Scientific Reports, 4, 6739, 2014.

Shi, C., Shen, M., Wu, X., Cheng, X., Li, X., Fan, T., Li, Z., Zhang, Y., Fan, Z., and Shi, F.: Growth response of alpine treeline forests to a warmer and drier climate on the southeastern Tibetan Plateau, Agricultural and Forest Meteorology, 264, 73-79, 2019.

Shi, H., Wang, B., Cook, E. R., Liu, J., and Liu, F.: Asian summer precipitation over the past 544 years reconstructed by merging tree rings and historical documentary records, Journal of Climate, 31, 7845-7861, 2018.

Sigdel, M., and Ikeda, M.: Spatial and temporal analysis of drought in Nepal using standardized precipitation index and its relationship with climate indices, Journal of Hydrology and Meteorology, 7, 59-74, 2010.

Singh, J., Park, W. K., and Yadav, R. R.: Tree-ring-based hydrological records for western Himalaya, India, since AD 1560, Climate Dynamics, 26, 295-303, 2006.

Stokes, M. A., and Smiley, T. L.: An introduction to tree-ring dating, University of Arizona Press, Tucson, USA, 1968.

Sun, C., and Liu, Y.: Tree-ring-based drought variability in the eastern region of the Silk Road and its linkages to the Pacific Ocean, Ecological Indicators, 96, 421-429, 2019.

Tejedor, E., Saz, M., Esper, J., Cuadrat, J., and de Luis, M.: Summer drought reconstruction in northeastern Spain inferred from a tree ring latewood network since 1734, Geophysical Research Letters, 44, 8492-8500, 2017.

Trenberth, K. E., Dai, A., van der Schrier, G., Jones, P. D., Barichivich, J., Briffa, K. R., and Sheffield, J.: Global warming and changes in drought, Nature Climate Change, 4, 17-22, 2014.

Treydte, K. S., Schleser, G. H., Helle, G., Frank, D. C., Winiger, M., Haug, G. H., and Esper, J.: The twentieth century was the wettest period in northern Pakistan over the past millennium. Nature, 440, 1179-1182, 2006.

Turner, D. P., Conklin, D. R., and Bolte, J. P.: Projected climate change impacts on forest land cover and land use over the Willamette River Basin, Oregon, USA, Climatic Change, 133, 335-348, 2015.

van der Schrier, G., Barichivich, J., Briffa, K., and Jones, P.: A scPDSI-based global data set of dry and wet spells for 1901–2009, Journal of Geophysical Research: Atmospheres, 118, 4025-4048, 2013.

van Oldenborgh, G. J., and Burgers, G.: Searching for decadal variations in ENSO precipitation teleconnections, Geophysical Research Letters, 32, L15701, 2005.

Vicente-Serrano, S.M., López-Moreno, J.I.: Nonstationary influence of the North Atlantic Oscillation on European precipitation. Journal of Geophysical Research-Atmospheres, 113, D20120, 2008.

Wang, B., Ding, Q., and Jhun, J. G.: Trends in Seoul (1778–2004) summer precipitation, Geophysical Research Letters, 33, L15803, 2006.

Wang, H., Chen, F., Ermenbaev, B., and Satylkanov, R.: Comparison of drought-sensitive tree-ring records from the Tien Shan of Kyrgyzstan and Xinjiang (China) during the last six centuries, Advances in Climate Change Research, 8, 18-25, 2017.

Wang, X., Brown, P.M., Zhang, Y., Song, L.: Imprint of the Atlantic multidecadal oscillation on tree-ring widths in northeastern Asia since 1568, PlOS ONE, 6, e22740, 2011.

Wang, X., Zhang, Q., Ma, K., and Xiao, S.: A tree-ring record of 500-year dry-wet changes in northern Tibet, China, Holocene, 18, 579-588, 2008.

Wang, Y., Li, S., Luo, D.: Seasonal response of Asian monsoonal climate to the Atlantic Mutidecadal Oscillation, Journal of Geophysical Research-Atmospheres 114, D02112, 2009.

Wigley, T. M., Briffa, K. R., and Jones, P. D.: On the average value of correlated time series, with applications in dendroclimatology and hydrometeorology, Journal of climate and Applied Meteorology, 23, 201-213, 1984.

Wiles, G. C., Solomina, O., D'Arrigo, R., Anchukaitis, K. J., Gensiarovsky, Y. V., and Wiesenberg, N.: Reconstructed summer temperatures over the last 400 years based on larch ring widths: Sakhalin Island, Russian Far East, Climate Dynamics, 45, 397-405, 2015.

Yadav, R. R., and Bhutiyani, M. R.: Tree-ring-based snowfall record for cold arid western Himalaya, India since AD 1460, Journal of Geophysical Research: Atmospheres, 118, 7516-7522, 2013.

Yadav, R. R.: Tree ring evidence of a 20th century precipitation surge in the monsoon shadow zone of the western Himalaya, India, Journal of Geophysical Research: Atmospheres, 116, 2011.

Yadav, R. R.: Tree ring–based seven-century drought records for the Western Himalaya, India, Journal of Geophysical Research: Atmospheres, 118, 4318-4325, 2013.

Yadav, R. R., Gupta, A. K., Kotlia, B. S., Singh, V., Misra, K. G., Yadava, A. K., and Singh, A. K.: Recent wetting and glacier expansion in the northwest Himalaya and Karakoram, Scientific Reports, 7, 6139, 2017.

Yao, J., and Chen, Y.: Trend analysis of temperature and precipitation in the Syr Darya Basin in Central Asia, Theoretical and Applied Climatology, 120, 521-531, 2015.

Yaqub, M., Eren, B., and Doğan, E.: Flood causes, consequences and protection measures in Pakistan, Disaster Science and Engineering, 1, 8-16, 2015.

Yu, J., Shah, S., Zhou, G., Xu, Z., and Liu, Q.: Tree-ring-recorded drought variability in the northern Daxing'anling Mountains of northeastern China, Forests, 9, 674, 2018.

Yu, M., Li, Q., Hayes, M. J., Svoboda, M. D., and Heim, R. R.: Are droughts becoming more frequent or severe in China based on the standardized precipitation evapotranspiration index: 1951–2010? International Journal of Climatology, 34, 545-558, 2014.

Zafar, M. U., Ahmed, M., Farooq, M. A., Akbar, M., and Hussain, A.: Standardized tree ring chronologies of *Picea smithiana* from two new sites of northern area Pakistan, World Applied Sciences Journal, 11, 1531-1536, 2010.

Zang, C., and Biondi, F.: Treeclim: an R package for the numerical calibration of proxy-climate relationships, Ecography, 38, 431-436, 2015.

Zhang, Q.-B., Evans, M. N., and Lyu, L.: Moisture dipole over the Tibetan Plateau during the past five and a half centuries, Nature Communications, 6, 8062, 2015.

Zhu, L., Li, Z., Zhang, Y., and Wang, X.: A 211-year growing season temperature reconstruction using tree-ring width in Zhangguangcai Mountains, Northeast China: linkages to the Pacific and Atlantic Oceans, International Journal of Climatology, 37, 3145-3153, 2017.

Figure captions

Fig. 1 Map of the weather stations (Drosh station) and sampling sites in the Chitral, HinduKush Mountains, Pakistan. Different colors represent the elevation changes of the study area.

Fig. 2 Monthly maximum, mean, minimum temperature (^{o}C) and total precipitation (mm) in the Drosh Weather Station (35.07° N, 71.78° E, 1465 m), Pakistan (1965-2013).

Fig. 3 The regional tree-ring width chronology from 1550 to 2017 in the Chitral, HinduKush Mountains, Pakistan. The gray area represents the sample depth.

Fig. 4 Pearson correlation coefficients between the tree-ring index of *C. deodara* and monthly total precipitation (1965-2013) and scPDSI (1960-2013) (a) and monthly maximum and minimum temperature (1965-2013) (b) from June of the previous year to September of the current year. Significant correlations (p<0.05) are denoted by asterisks. The "previous" and "current" represents the previous and current year, respectively.

Fig. 5 The scPDSI reconstruction in the Chitral HinduKush Mountain, Pakistan. (a) Comparison between the reconstructed (black line) and actual (red line) scPDSI; (b) The variation of annual (black solid line) and 11-year moving average (red bold line) Mar-Aug scPDSI from 1593 to 2016 with mean vale ± one standard deviation (black dash lines).

Fig. 6 Comparison of our PDSI reconstruction (a) with the precipitation reconstruction (tree-ring $\delta^{18}O$) of Treydte et al. (2006) (b) in northern Pakistan. Purple and brown shaded areas represent the consistent wet and dry periods in the two reconstructions, respectively. Two correlation coefficients (r = -0.24 and r = -0.11) are the correlation of two original annual resolution reconstruction series and two 11-year moving average series, respectively.

Fig. 7 The Multi-taper method spectrums of the reconstructed scPDSI from 1593 to 2016. Red and green line represents the 95% and 99% confidence level, respectively. The figures above the significant line represents the significant periods of drought at 95% confidence level.

Fig. 8 (a) Spatial correlation between the actual May-August PDSI and the reconstructed May-August scPDSI (1901-2017). (b) The wavelet analysis of the reconstructed scPDSI in the Chitral HinduKush Ranges, Pakistan. The 95% significance level against red noise was shown as a black contour.

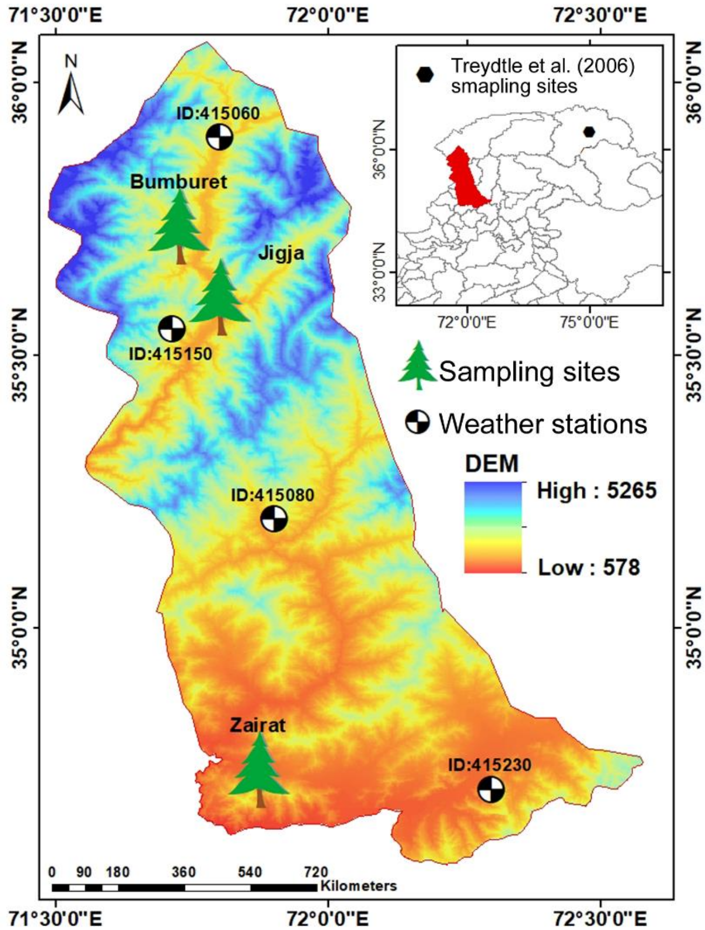

Fig. 1 Map of the weather stations (Drosh station) and sampling sites in the Chitral, HinduKush Mountains, Pakistan. Different colors represent the elevation changes of the study area.

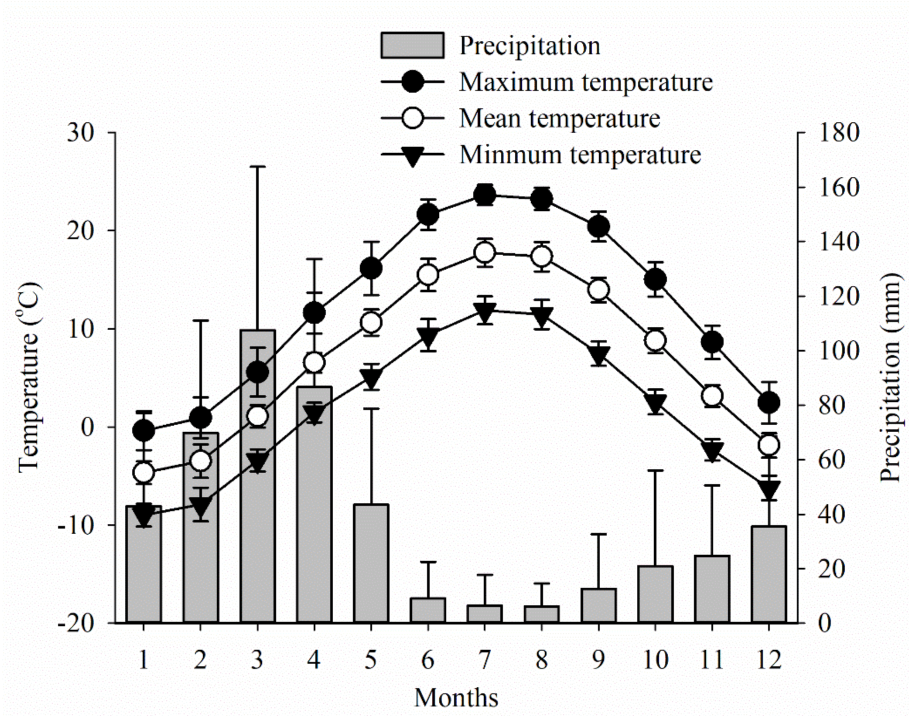

Fig. 2 Monthly maximum, mean, minimum temperature (°C) and total precipitation (mm) in the Drosh Weather Station (35.07° N, 71.78° E, 1465.0 m), Pakistan (1965-2013).

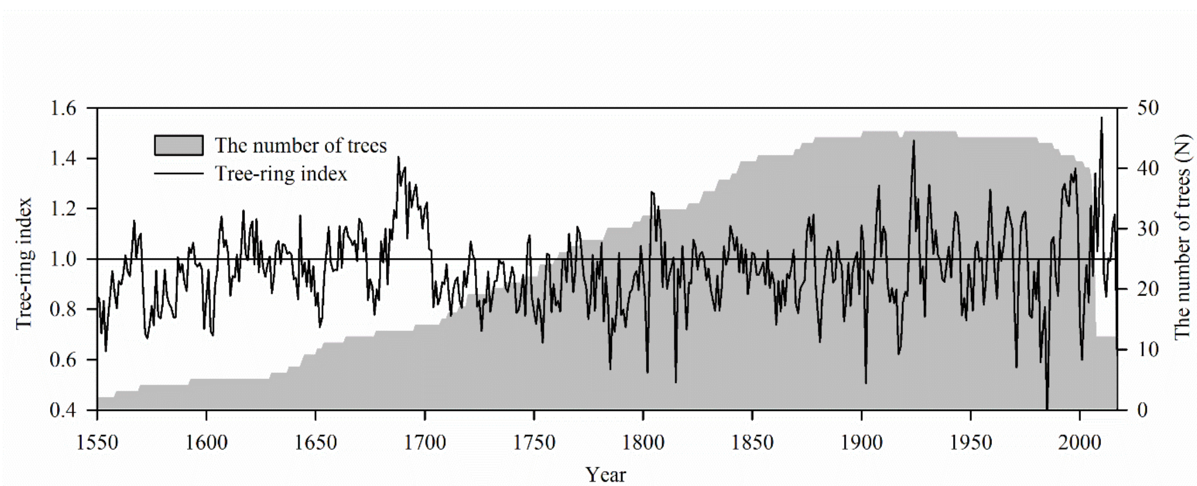

Fig. 3 The regional tree-ring width chronology from 1550 to 2017 in the Chitral, HinduKush Mountains, Pakistan. The gray area represents the sample depth.

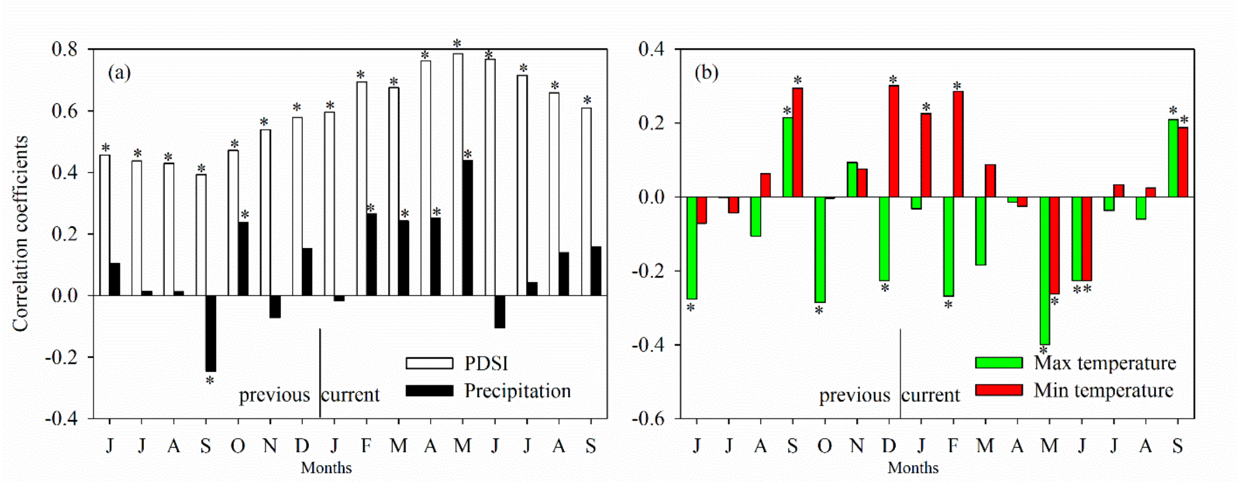

Fig. 4 Pearson correlation coefficients between the tree-ring index of *C. deodara* and monthly total precipitation (1965-2013) and scPDSI (1960-2013) (a) and monthly maximum and minimum temperature (1965-2013) (b) from June of the previous year to September of the current year. Significant correlations (p<0.05) are denoted by asterisks. The "previous" and "current" represents the previous and current year, respectively.

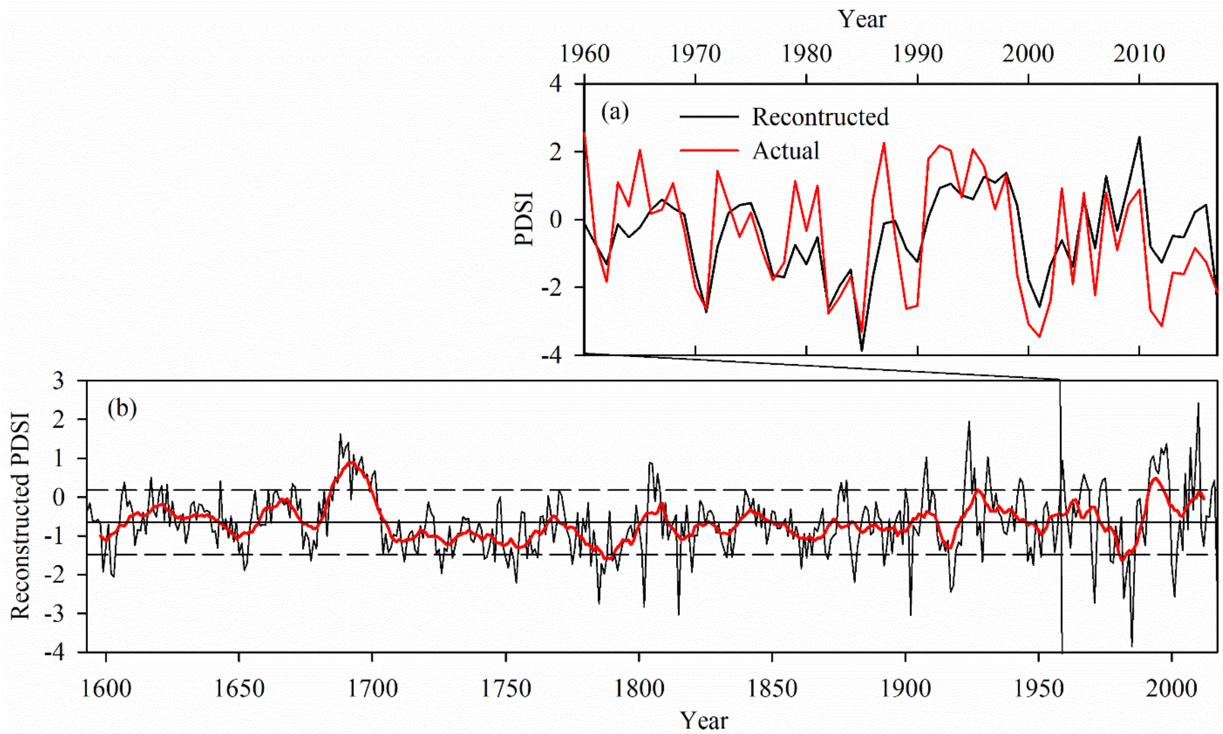

Fig. 5 The scPDSI reconstruction in the Chitral HinduKush Mountain, Pakistan. (a) Comparison between the reconstructed (black line) and actual (red line) scPDSI; (b) The variation of annual (black solid line) and 11-year moving average (red bold line) Mar-Aug scPDSI from 1593 to 2016 with mean vale ± one standard deviation (black dash lines).

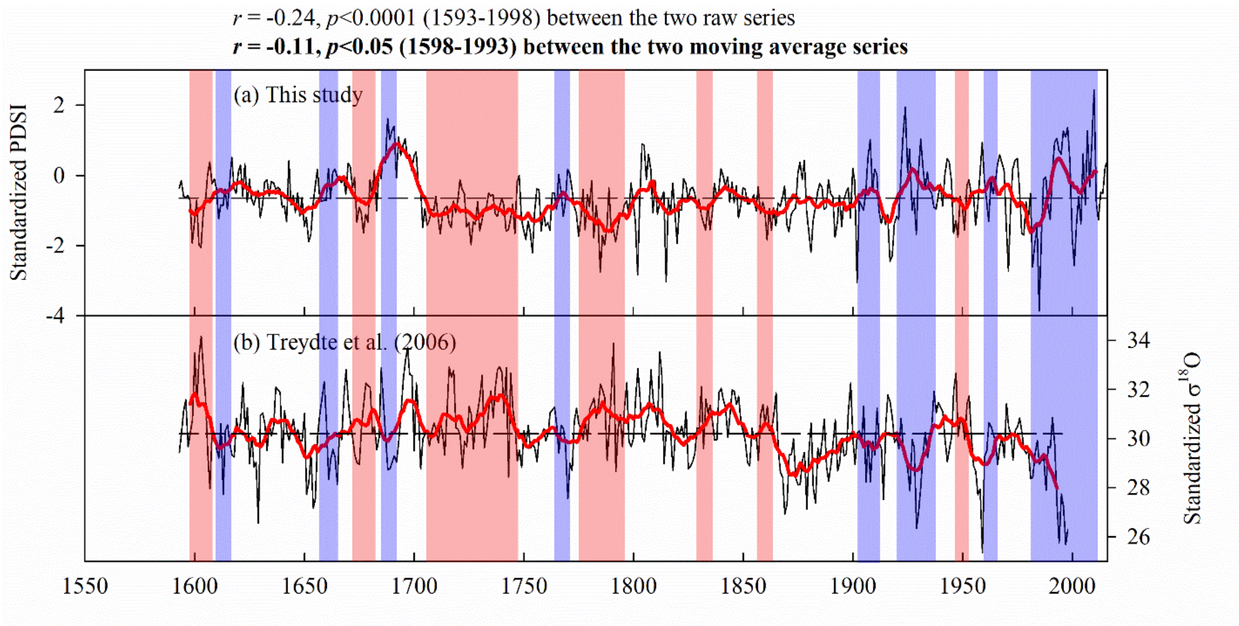

Fig. 6 Comparison of our PDSI reconstruction (a) with the precipitation reconstruction (tree-ring $\delta^{18}O$) of Treydte et al. (2006) (b) in northern Pakistan. Purple and brown shaded areas represent the consistent wet and dry periods in the two reconstructions, respectively. Two correlation coefficients (*r* = -0.24 and *r* = -0.11) are the correlation of two original annual resolution reconstruction series and two 11-year moving average series, respectively.

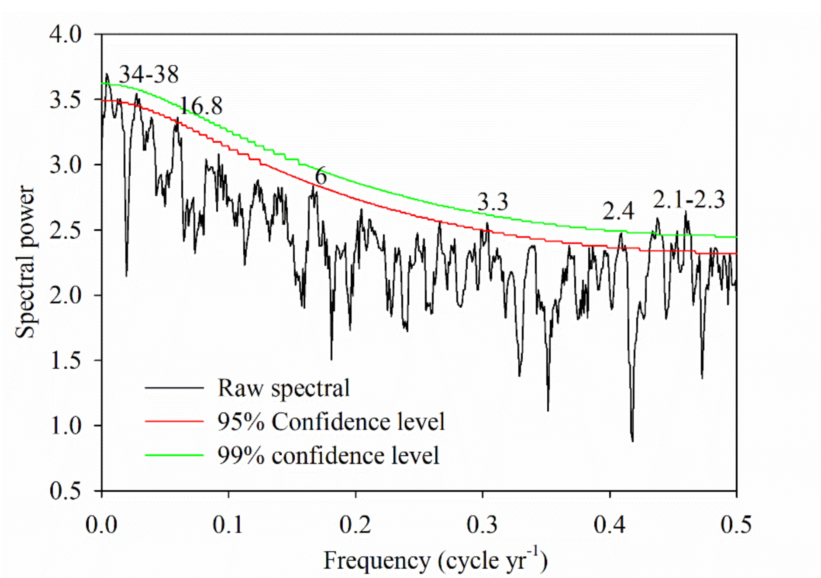

Fig. 7 The Multi-taper method spectrums of the reconstructed scPDSI from 1593 to 2016. Red and green line represents the 95% and 99% confidence level, respectively. The figures above the significant line represents the significant periods of drought at 95% confidence level.

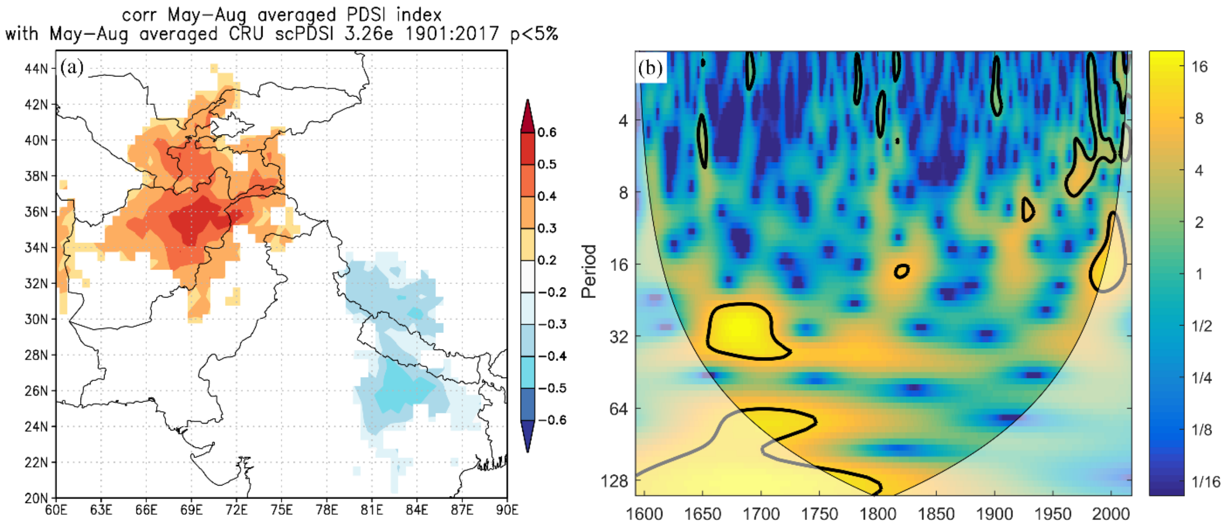

Fig. 8 (a) Spatial correlation between the actual May-August PDSI and the reconstructed May-August scPDSI (1901-2017). (b) The wavelet analysis of the reconstructed scPDSI in the Chitral HinduKush Ranges, Pakistan. The 95% significance level against red noise was shown as a black contour.

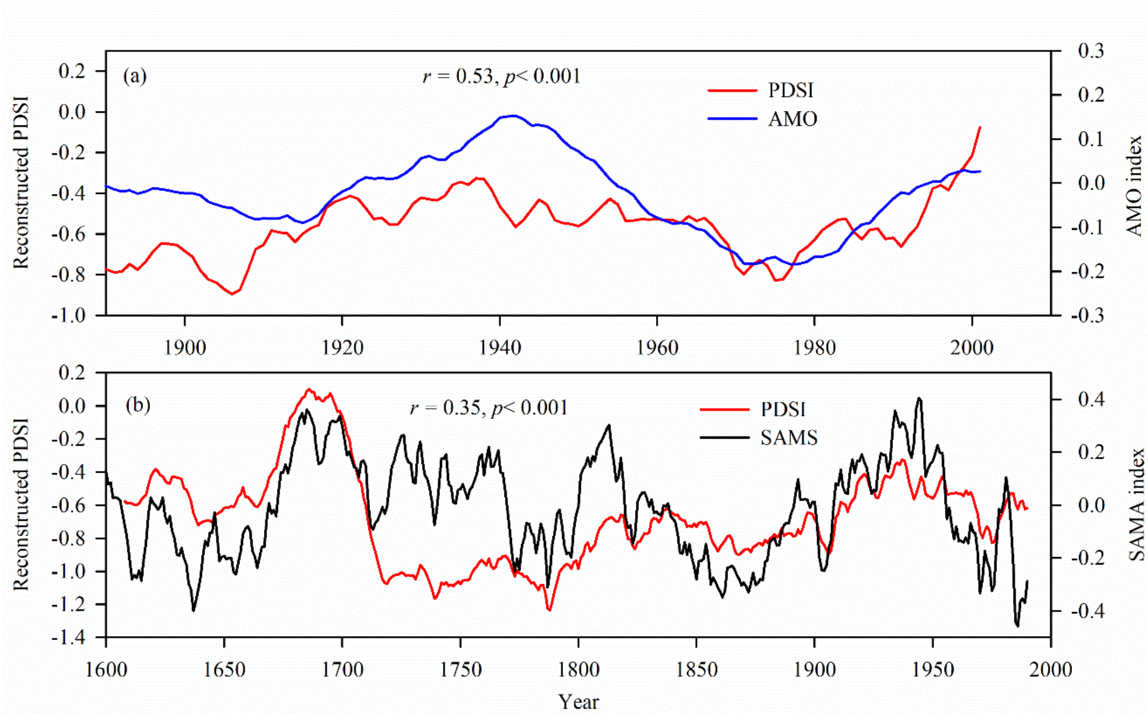

Fig. 9 (a) Comparison of the 31-year moving average series between the reconstructed Mar-Aug scPDSI and the AMO index during the common period (1890-2001); (b) Comparison of the 31-year moving average series between the reconstructed Mar-Aug scPDSI and the JJA-SAMS during the common period (1608-1990).

Table 1. Statistical test for the tree-ring reconstruction of March-August PDSI in Chitral HinduKush Range of northern Pakistan based on a split calibration-verification procedure.

Calibrations	*r*	R^2	Verification	RE	CE	ST	DW	RMSE	PMT
1960-2016	0.70	0.49	—	0.44	—	(43, 14)*	1.06*	1.21	10.0*
1989-2016	0.82	0.67	1960-1988	0.61	0.62	(23, 6)*	1.0*	1.72	5.80*
1960-1988	0.73	0.53	1989-2016	0.64	0.62	(24, 4)*	0.98*	1.56	7.42*

Notes: RE-Reduction of error, CE-Coefficient of efficiency, ST-Sign test, DW-Durbin-Watson test, RMSE-Root mean square error, PMT-Product means test.